Visibility Laboratory
University of California
Scripps Institution of Oceanography
San Diego 52, California

# MULTIPLIER PHOTOTUBE

# SECONDARY EMISSION CHARACTERISTICS

Richard L. Ensminger

March 1959
Index Number NS 714-100

Bureau of Ships
Contract NObs-72092

SIO Reference 59-11

Approved:

Seibert Q. Duntley

Seibert Q. Duntley, Director
Visibility Laboratory

Approved for Distribution:

Roger Revelle

Roger Revelle, Director
Scripps Institution of Oceanography

SIO Ref. 59-11


## Abstract

This paper suggests a method for fitting the secondary emission characteristic of multiplier phototubes to a general equation for secondary emission from metalic surfaces. An analysis of this equation affords an explanation of the observed fact that multiplier phototube gain is proportional to the n-th power of the dynode supply voltage over a limited range.

The technique followed was to develop an approximate form of the theoretical secondary emission characteristic, and then to correlate this analysis with an experimental determination of this characteristic for a specific 931-A multiplier phototube.

SIO Ref. 59-11

## TABLE OF CONTENTS

## Section 1

## Introduction

This paper suggests a method for curve fitting to the dynode characteristics of a 931-A multiplier phototube. An examination of the ninth dynode characteristic is also made to determine to what extent it exhibits an n-th power characteristic.

Interest in this subject at the Visibility Laboratory has been stimulated by development work on logarithmic photometers. Of major importance in this work is the characteristic of the gain versus the dynode voltage curve. Of special interest is the general n-th power behavior exhibited by multiplier phototubes. What is meant by this is that the gain can be expressed as the dynode voltage raised to some power (usually between 6 and 7 for the 931-A). If this characteristic could be relied upon, a direct logarithmic conversion of the dynode voltage would yield a signal linearly proportional to the logarithm of the input flux (providing the anode current is held at a constant value).

To answer these questions the dynode characteristics of a 931-A were obtained experimentally. It was found that this characteristic was in agreement with theoretical considerations and that an n-th power behavior could be predicted on the basis of this theory.

## Section 2

## Theoretical Secondary Emission Characteristic

Bruining makes reference to an analytic expression for secondary emission from metals.[1] This defines the secondary emission ratio, $\delta$, normalized to the maximum secondary emission, $\delta_{max}$, as a function of the excitation potential, $V_p$, normalized to that potential which results in the maximum secondary emission, $V_{pmax}$.

$$\frac{\delta}{\delta_{max}} = 1.85\, e^{-r^2} \int_0^r e^{y^2} dy \qquad (1)$$

$$r = \frac{0.92\, V_p}{V_{pmax}}$$

This curve has been plotted in Figure 1.

The above equation is difficult to handle analytically and apply to experimental results. To obtain a simplified expression for secondary emission the terms can be expanded in a power series.

$$\int_0^r e^{y^2} dy = r + \frac{r^3}{3} + \frac{r^5}{5 \cdot 2!} + \frac{r^7}{7 \cdot 3!} + \cdots$$

$$e^{-r^2} = 1 - r^2 + \frac{r^4}{2!} - \frac{r^6}{3!} + \cdots$$

---

[1] H. Bruining, Physics and Applications of Secondary Electron Emission (McGraw-Hill Book Company, Inc., New York, 1954), pp 78-81.

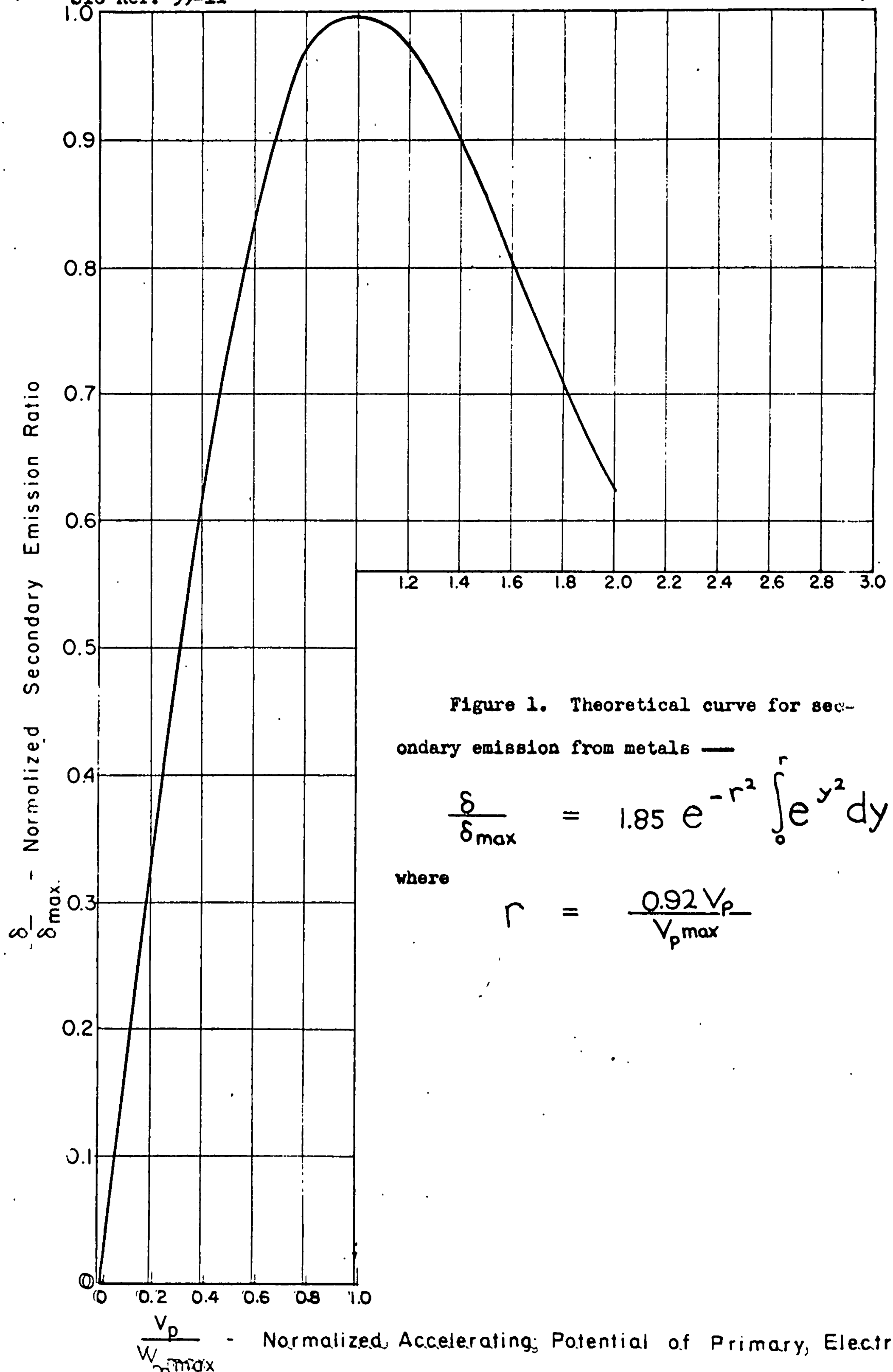


**Figure 1. Theoretical curve for secondary emission from metals —**

$$\frac{\delta}{\delta_{max}} = 1.85\, e^{-r^2} \int_0^r e^{y^2} dy$$

**where**

$$r = \frac{0.92\, V_p}{V_{p\,max}}$$

Taking only the first two terms in each series and forming the product one obtains,

$$e^{-r^2}\int_0^r e^{y^2}dy \approx r(1-\tfrac{2}{3}r^2)-\frac{r^5}{3}$$

$$\approx r(1-\tfrac{2}{3}r^2)$$

This will hold for $r << 1$. Hence for small values of r, which means for excitation voltages much smaller than $V_{pmax}$, an approximate equation for secondary emission can be written as follows:

$$\frac{\delta}{\delta_{max}} \approx 1.85\left(\frac{0.92\,V_p}{V_{pmax}}\right)\left[1-\frac{2}{3}\left(\frac{0.92\,V_p}{V_{pmax}}\right)^2\right] \qquad (2)$$

Computations of $\frac{\delta}{\delta max}$ were made from the above equation and the results compared with the exact expression. Excellent agreement was found up to $\frac{V_p}{V_{pmax}} = 0.5$.

## Section 3

## Experimental Verification

To check the validity of the approximate expression derived in the preceeding section, a secondary emission curve for the nintn dynode of a 931-A was obtained in the laboratory. The direct use of the theoretical equation necessitates a knowledge of the constants $V_{pmax}$ and $\delta_{max}$. To get around this difficulty, the experimental data was matchea to the theoretical curve as follows.

a. It was assumed that $V_p = V_d - V_o$. Here $V_d$ is the dynode voltage per stage, and $V_o$ is an experimental constant. The need for assuming a $V_o$ became apparent when it was found that there was some secondary emission even with zero dynode voltage.

b. The initial slope of the experimental data was matched to the initial slope of the theoretical curve.

c. A match point was selected at a fairly high value of dynode voltage.

Based on these considerations, the mathematical procedure will now be summarized.

The experimental data is to be fitted to the curve,

$$\delta = 1.85\,\delta_{max}\left[\frac{0.92(V_d-V_o)}{V_{pmax}}\right]\left\{1-\frac{2}{3}\left[\frac{0.92(V_d-V_o)}{V_{pmax}}\right]^2\right\} \qquad (3)$$

From the experimental data curve one obtains

$\delta'(0)$, the initial slope, and

$V_o$, the intersection of the extended data curve with the voltage axis.

A match point is selected ( $\delta_1, V_{d1}$).

The values of $V_{p\,max}$ and $\delta_{max}$ are now computed from the relationships,

$$V_{p\,max} = \frac{0.92(V_{d1} - V_o)}{\sqrt{\frac{3}{2}\left[1 - \frac{\delta_1}{\delta'(0)(V_{d1} - V_o)}\right]}}$$

$$\delta_{max} = \frac{\delta'(0)\ V_{p\,max}}{1.7}$$

The curve in Figure 2 shows the result of this correlation. This close correlation between the computed curve and the experimental data suggests that equation (3) may be a valid description of dynode secondary emission for normal dynode voltages.

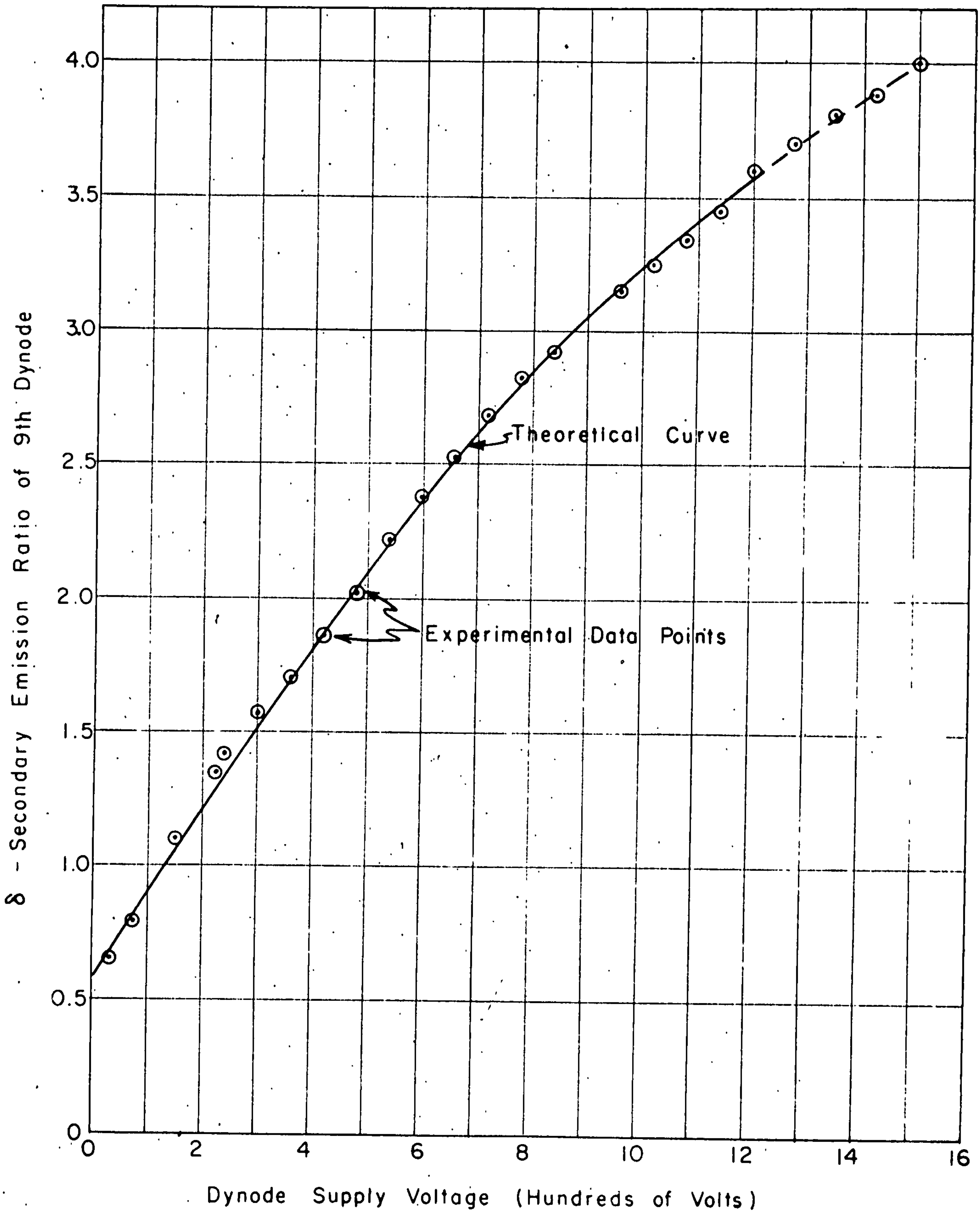


**Figure 2.** Correlation of the experimental secondary emission data from a 931-A (#323) with an approximation to the theoretical secondary emission curve,

$$\delta = 1.85\,\delta_{max}\left[\frac{0.92(V_d - V_o)}{V_{p\,max}}\right]\left\{1 - \frac{2}{3}\left[\frac{0.92(V_d - V_o)}{V_{p\,max}}\right]^2\right\}$$

$V_{p\,max}$ = 261 volts, $V_o$ = -20.3 volts, $\delta_{max}$ = 4.45.

## Section 4

## Logarithmic Characteristic

It has long been observed that the gain versus dynode voltage characteristic of a multiplier phototube tends to be a straight line when plotted on log-log paper. That is to say that the gain is related to the voltage by an equation of the form,

$$g = k V_d^{\,n}$$

where

$$g = \text{multiplier phototube gain}$$
$$V_d = \text{dynode voltage per stage}$$
$$k, n = \text{constants}$$

As evidence of this apparent behavior three charts (Figures 3, 4 and 5) have been included. Figure 3 shows the gain characteristic of a 931-A as published in the RCA Tube Manual, while Figure 4 shows the gain characteristic of the 931-A used in this experiment. Both curves are remarkably straight. In fact the tube manual curve is to all intents and purposes a straight line, whereas the experimental curve deviates from linearity only in the last log cycle. Figure 5 shows a number of 5819 characteristics taken over a period of time at the Visibility Laboratory.

This present section is an attempt to show that the theoretical relationship derived from Bruining's Equation [equation (3)] exhibits n-th power characteristics over a limited range — ~~providing~~ proving there is a theoretical justification to the n-th power characteristic observed experimentally.

To obtain a correlation between an n-th power curve and the approximation of the secondary emission curve, a Taylor series expansion

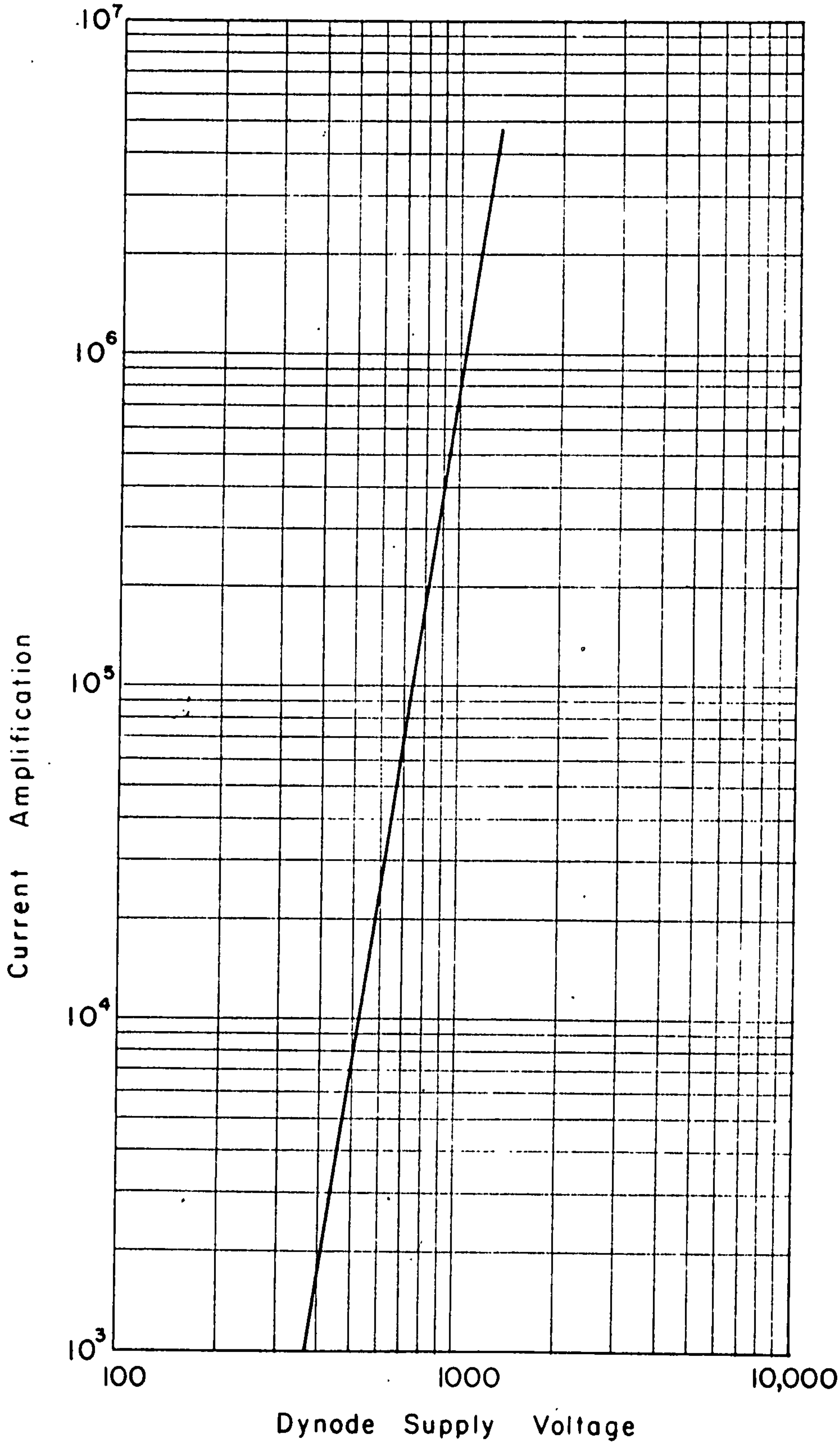


**Figure 3.** Current amplification curve for the 931-A shown in the RCA Tube Manual, closely approximated by the expression

$$g = 1.91 \times 10^{-8} V_d^{6.66}$$

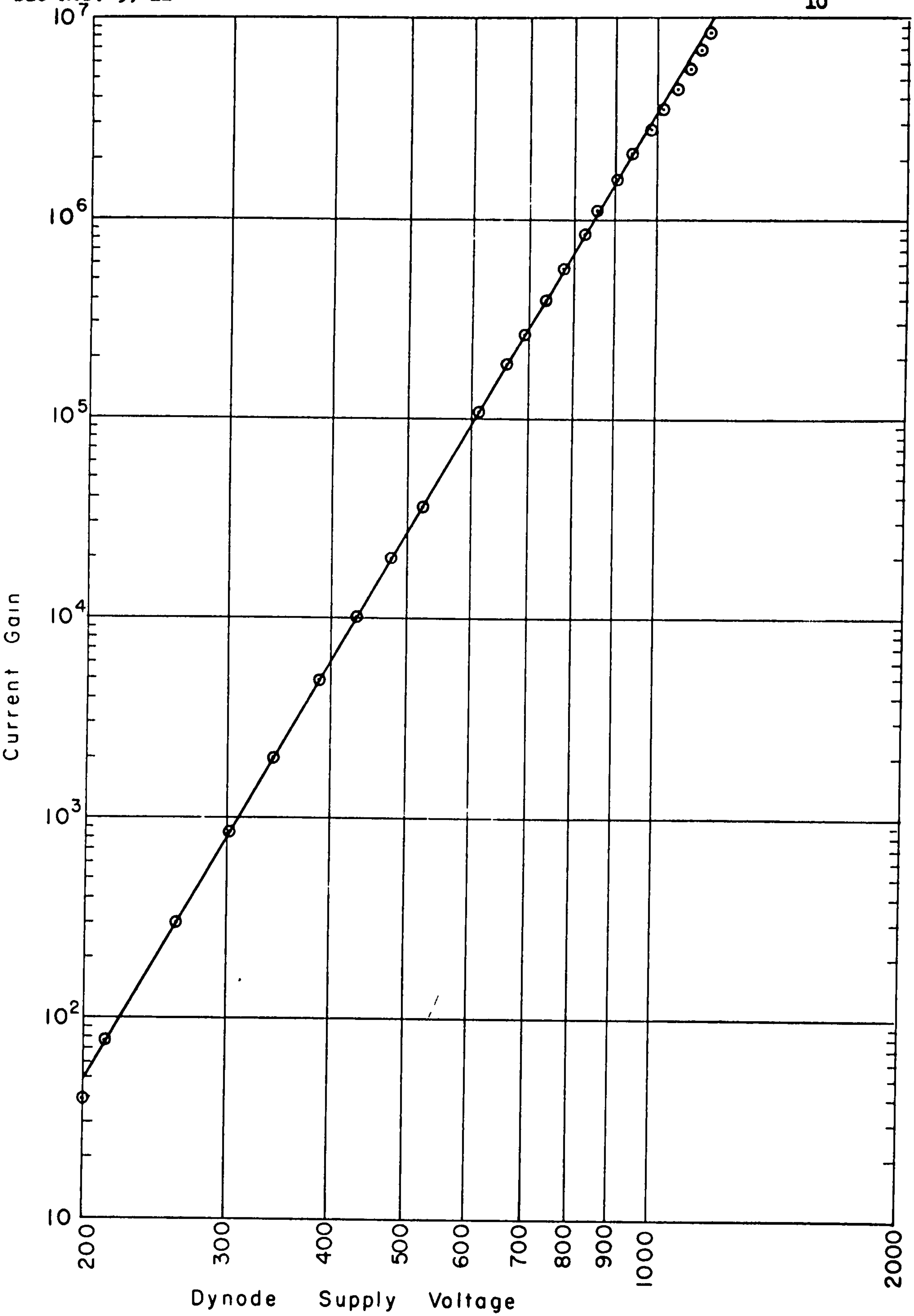


Figure 4. Current amplification characteristic obtained experimentally for a 931-A (#323).

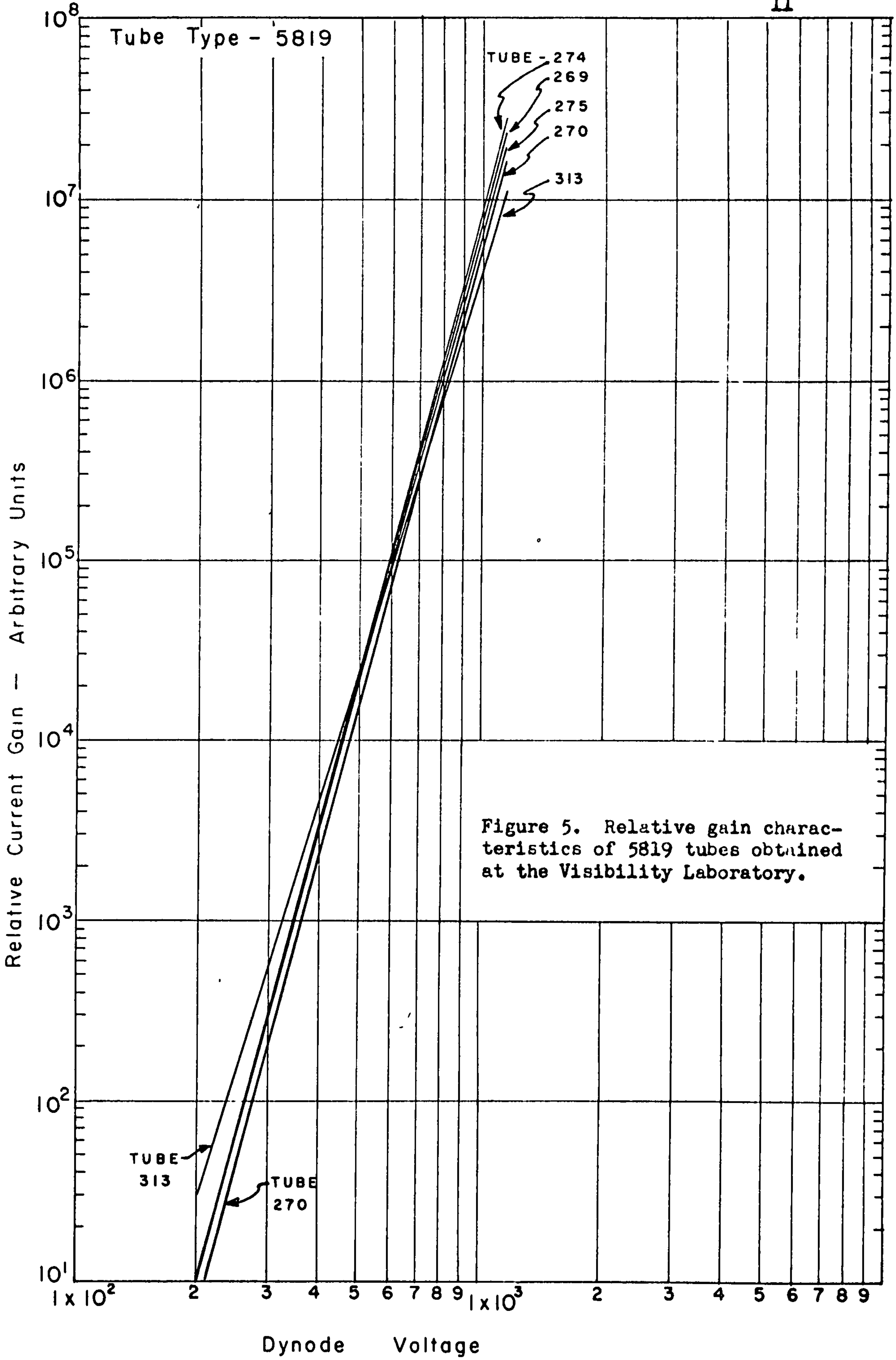


Figure 5. Relative gain characteristics of 5819 tubes obtained at the Visibility Laboratory.

of the two equations will be made about some arbitrary point a.

Expanding the secondary emission curve [equation (3)] in a Taylor expansion,

$$\delta = 1.85\,\delta_{max}\left\{\left(a-\frac{0.92\,V_o}{V_{pmax}}\right)\left[1-\frac{2}{3}\left(a-\frac{0.92\,V_o}{V_{pmax}}\right)^2\right]+\left[1-2\left(a-\frac{0.92\,V_o}{V_{pmax}}\right)^2\right]\cdot\right.$$

$$\left.\left(\frac{0.92V_d}{V_{pmax}}\right)-4\left(a-\frac{0.92\,V_o}{V_{pmax}}\right)\left(\frac{0.92\,V_d}{V_{pmax}}\right)^2-4\left(\frac{0.92V_d}{V_{pmax}}\right)^3\right\}$$

Assuming that the secondary emission can be expressed in terms of an n-th power relationship of the form,

$$\delta = 1.85\,\delta_{max}\,B\left(\frac{0.92\,V_d}{V_{pmax}}\right)^n \tag{4}$$

and expanding about the point a.

$$\frac{\delta}{1.85\,\delta_{max}} = Ba^n + Bna^{n-1}\left(\frac{0.92\,V_d}{V_{pmax}}\right) + Bn(n-1)a^{n-2}\left(\frac{0.92\,V_d}{V_{pmax}}\right)^2 +$$

$$Bn(n-1)(n-2)a^{n-3}\left(\frac{0.92\,V_d}{V_{pmax}}\right)^3 + \cdots$$

Since there are only three independent variables, B, n and a, the best match that can be made between the two equations consists of equating the coefficients of the first three terms in the series. A set of three simultaneous equations could be set up in this way; however a solution is difficult because of the transcendental nature of the equations. The procedure that was adopted was to select a value of a; then compute B and n from the equations

$$n = \frac{a\left[1-2\left(a-\frac{0.92\,V_o}{V_{p\,max}}\right)^2\right]}{\left(a-\frac{0.92\,V_o}{V_{p\,max}}\right)\left[1-\frac{2}{3}\left(a-\frac{0.92\,V_o}{V_{p\,max}}\right)^2\right]}$$

$$B = \frac{\left(a-\frac{0.92\,V_o}{V_{p\,max}}\right)\left[1-\frac{2}{3}\left(a-\frac{0.92\,V_o}{V_{p\,max}}\right)^2\right]}{a^n}$$

The correct value of a was then found from the intersection of the two functions,

$$a_1(B,n) = -4\left(a-\frac{0.92\,V_o}{V_{p\,max}}\right)$$

and

$$a_2(B,n) = Bn(n-1)a^{n-2}$$

Using the constants $\delta_{max} = 4.45$, $V_{p\,max} = 261$ volts, and $V_o = -20.3$ volts, the corresponding values of n and B were found to be $n = 0.663$ and $B = 0.752$. These are the values of n and B which also satisfy the equation

$$Bn(n-1)a^{n-2} = -4\left(a-\frac{0.92\,V_o}{V_{p\,max}}\right)$$

The value of a satisfying this equation is $a = 0.228$, which means that the Taylor series is expanded about the point

$$V_d = \frac{V_{p\,max}}{0.92}\,a = 64.7 \text{ volts}$$

Thus we have approximated the secondary emission curve by the equation

$$\delta = 1.85\,\delta_{max}\,(0.752)\left(\frac{0.92\,V_d}{V_{p\,max}}\right)^{0.663} \tag{5}$$

Figure 6 shows the correspondence between these curves. The agreement is quite close from 25 volts to 115 volts.

Figure 7 shows the effect of raising both curves to the ninth power, which would be comparable to obtaining the overall photomultiplier tube gain if each dynode had the same $\delta$ versus $V_d$ characteristic. The agreement between the two curves is still quite close over four log cycles. The theoretical secondary emission curve also exhibits the same characteristics of decreasing slope at either end of the dynode voltage range which is characteristic of experimental data.

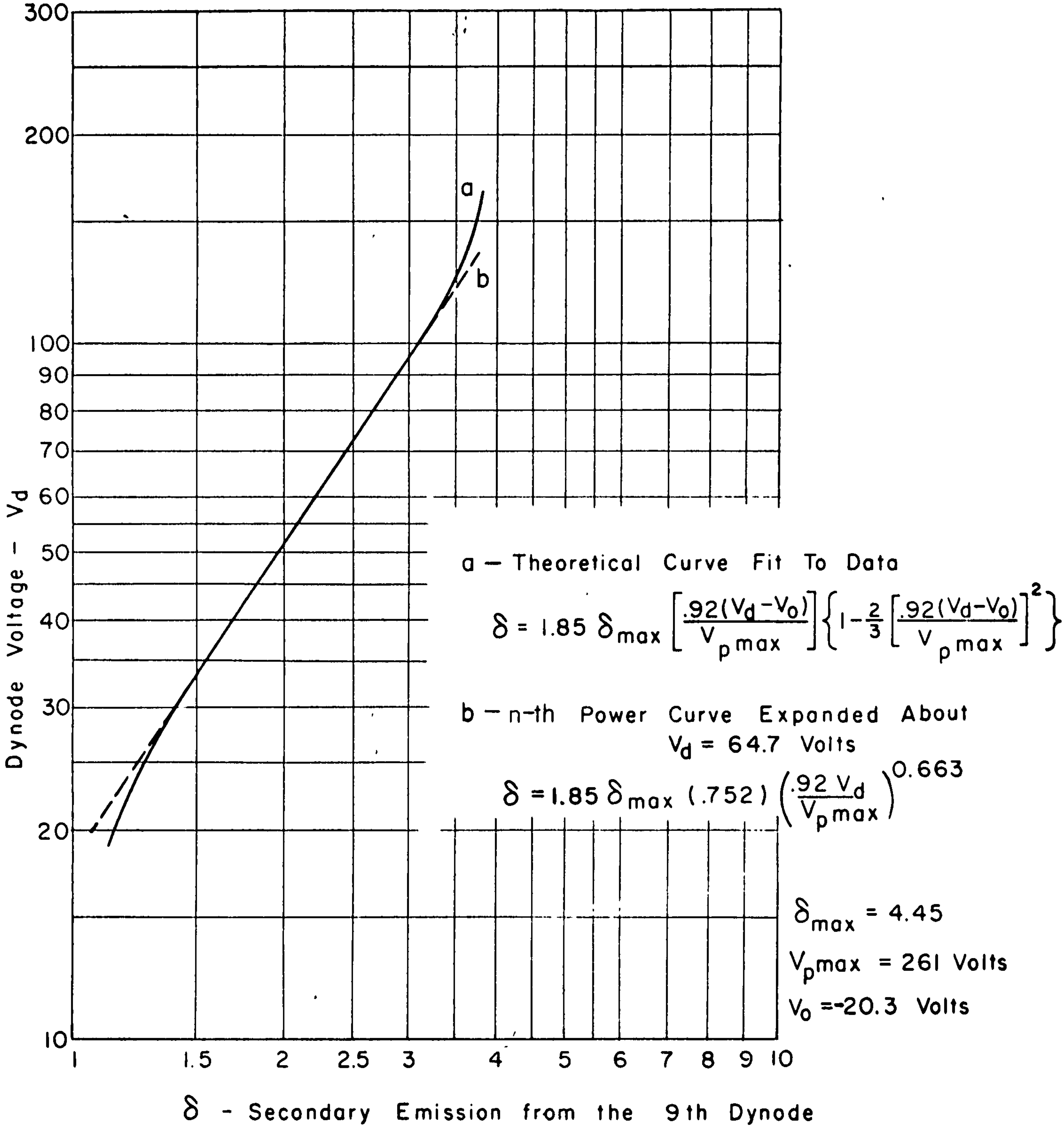


Figure 6. Illustration of the closeness of fit of an n-th power curve expanded about $V_d$ = 64.7 to the theoretical secondary emission curve.

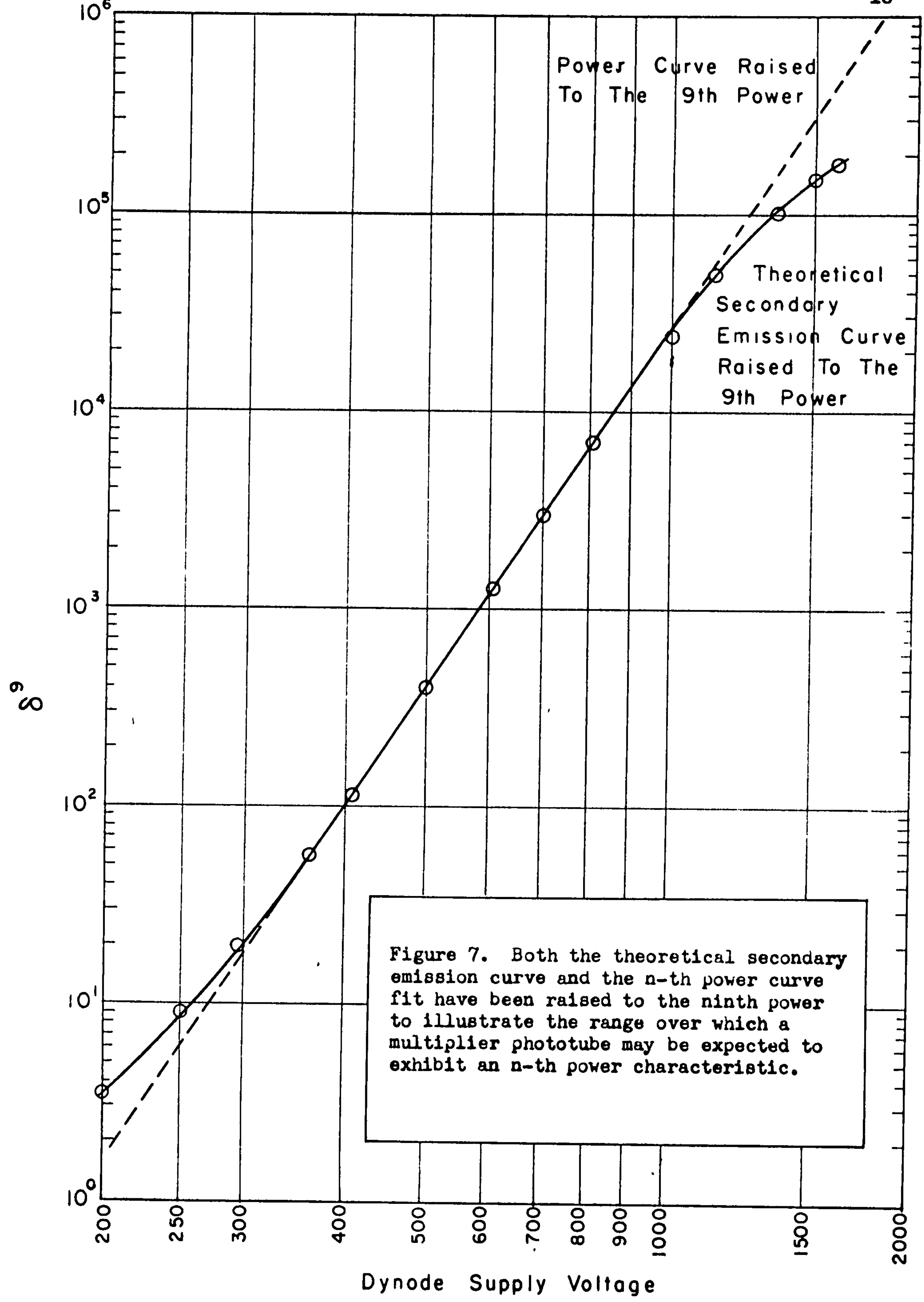


Figure 7. Both the theoretical secondary emission curve and the n-th power curve fit have been raised to the ninth power to illustrate the range over which a multiplier phototube may be expected to exhibit an n-th power characteristic.

## Section 5

## Secondary Emission Characteristics of the Other Dynodes

Part of the original goal of the experiment was to obtain a complete secondary emission characteristic for each dynode. This was done by connecting the tube to an unusually low impedance dynode string and measuring each dynode current individually. The dynode supply voltage was then varied over as wide a range as was practical while readjusting the light source each time to yield the same anode current. Figure 8 is a schematic which illustrates the circuit and the resulting currents. Computation of the individual secondary emission ratios was made from the relationship

$$\delta_n = \frac{\sum_{j=0}^{n} i_j}{\sum_{j=0}^{n-1} i_j}$$

and the alternate relationship

$$\delta_n = \frac{i_{10} - i_9 - i_8 - i_7 - \cdots - i_{n+1}}{i_{10} - i_9 - i_8 - i_7 - \cdots - i_{n+1} - i_n}$$

Two other useful relationships are

$$i_{10} = \sum_{j=0}^{9} i_j$$

and

$$i_{10} = (\delta_1 \delta_2 \delta_3 \delta_4 \cdots \delta_9) i_c$$

Because of the low currents encountered, the highest value of dynode supply voltage for which reliable readings could be made was 600 volts or 66.7 volts per stage. The corresponding values of secondary

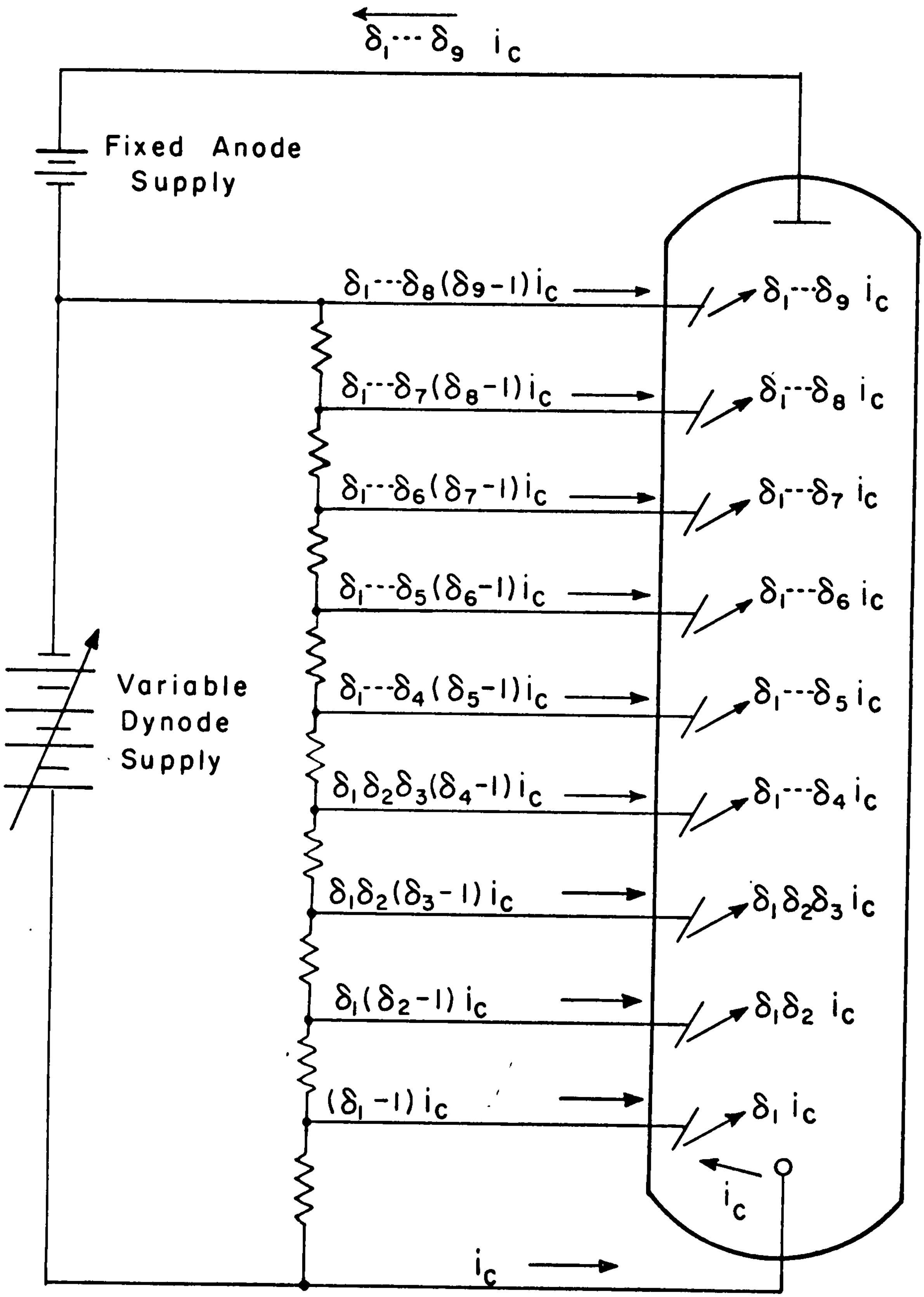


Figure 8. Multiplier Phototube Schematic

emission computed from these readings are shown in Figure 9. A plot of the characteristics (Figure 10) has also been included. It can be seen from the figure that the value of the secondary emission becomes increasingly unreliable for the lower dynodes. This is because of the small currents encountered. Not having the complete characteristic for these dynodes, it was not possible to fit each one individually to the theoretical curve as was done for the ninth dynode (see Figure 7). The most striking fact about the characteristics is that they exhibit distinctly different slopes; hence, the parameters $\delta_{max}$ and $V_{p max}$ apparently vary from dynode to dynode.

| Dynode Supply Voltage | $\delta_1$ | $\delta_2$ | $\delta_3$ | $\delta_4$ | $\delta_5$ | $\delta_6$ | $\delta_7$ | $\delta_8$ | $\delta_9$ |
|---|---|---|---|---|---|---|---|---|---|
| 225 | 1.80 | 1.37 | 1.57 | 1.24 | 1.54 | 1.26 | 1.68 | 1.23 | 1.35 |
| 300 | 2.42 | 1.78 | 2.00 | 1.66 | 1.82 | 1.65 | 2.01 | 1.52 | 1.55 |
| 375 | 2.67 | 1.94 | 2.25 | 2.02 | 2.15 | 2.07 | 2.35 | 1.87 | 1.76 |
| 450 | 3.09 | 2.47 | 2.38 | 2.50 | 2.54 | 2.57 | 2.71 | 2.22 | 1.99 |
| 525 | 3.33 | 2.60 | 3.15 | 2.85 | 2.92 | 3.19 | 3.06 | 2.59 | 2.21 |
| 600 | 3.00 | 2.67 | 3.25 | 3.08 | 3.00 | 3.63 | 3.30 | 2.85 | 2.41 |
| 675 | 5.00 | 3.40 | 3.47 | 3.44 | 3.17 | 4.05 | 3.77 | 3.08 | 2.59 |

**Figure 9.** Table of values of secondary emission for tne dynodes of a 931-A(#323) obtained experimentally.

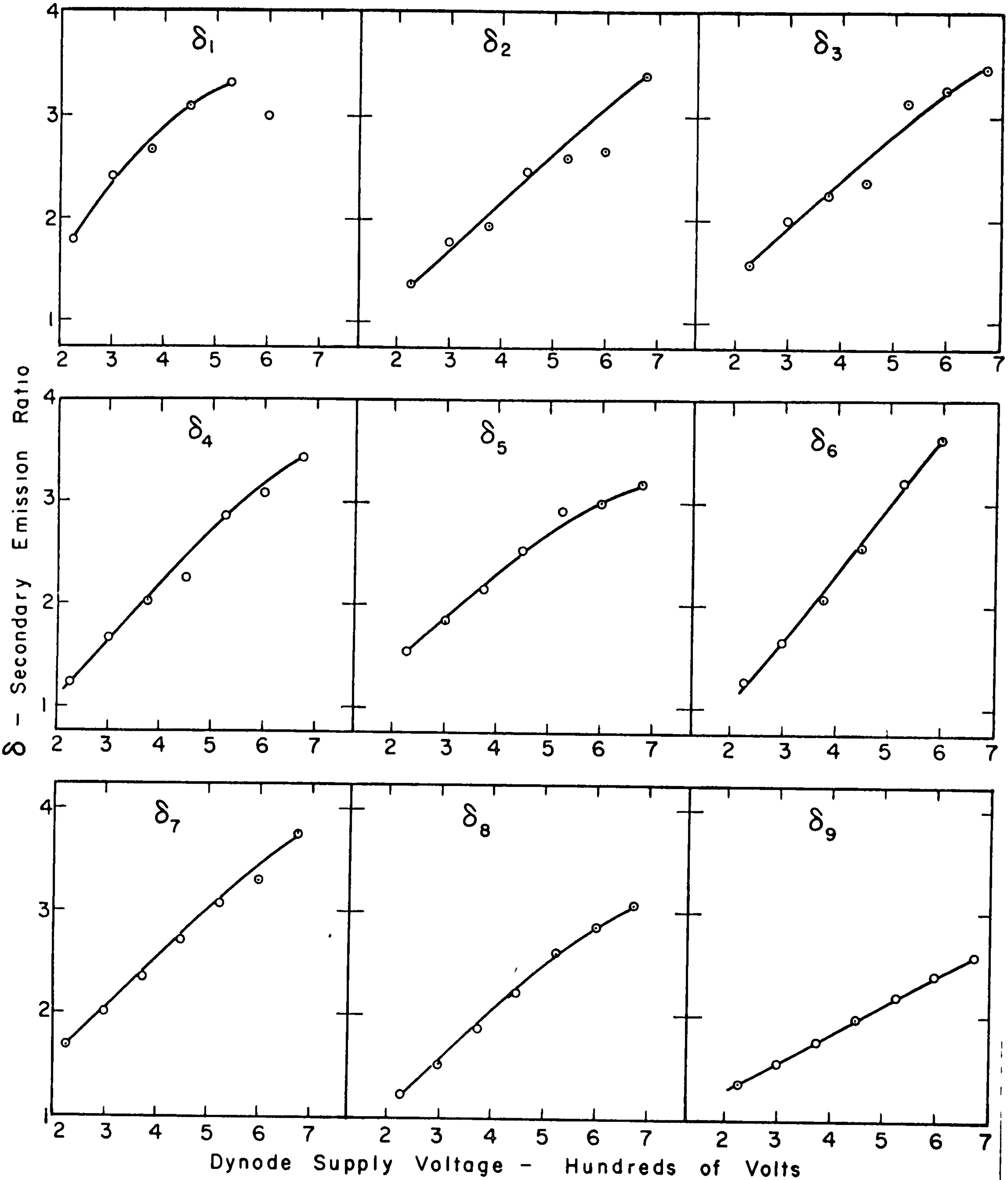


**Figure 10.** Secondary emission characteristics of the dynodes in a 931-A(#323) obtained experimentally.

## Section 6

## Summary

The steps followed in this paper were:

a. To develop an approximate expression for secondary emission based upon a theoretical equation quoted by Bruining.

b. To modify the form of this expression to fit experimental data.

c. To show that the theoretical secondary emission curve behaves like an n-th power curve over a limited range.

Apparently secondary emission is so affected by surface irregularities, impurities, and other detailed characteristics of the metal surface, that an exact expression based upon theory is not yet available. However, the expression quoted by Bruining is a gross approximation that describes the general behavior of secondary emission from metallic surfaces. It was shown in this paper that insofar as a dynode surface follows this characteristic, an n-th power behavior can be predicted over about four log cycles. The data from the multiplier phototube used in this experiment fit the theoretical curve quite well, although there may be tubes which cannot be made to fit this theoretical characteristic.

To summarize the conclusions arrived at,

1. Secondary emission characteristics vary widely from dynode to dynode (see Figure 10).

2. It can be predicted from theory that secondary emission from dynodes can be grossly defined by equation (3) up to dynode voltages of 150 volts.

3. There is a theoretical justification for the observed n-th power behavior of the photomultiplier gain curve characteristic.

# BIBLIOGRAPHY

V. K. Zworykin, G. A. Morton and L. Malter, "The Secondary Emission Multiplier — A New Electronic Device," Proc. I.R.E., Vol. 24, p. 351, March, 1936.

V. K. Zworykin and J. A. Rajchman, "The Electrostatic Electron Multiplier," Proc. I.R.E., Vol. 27, p. 558, September, 1939.

R. B. Janes and A. M. Glover, "Recent Developments in Phototubes," RCA Review, Vol. 6, p. 43, July, 1941.

G. A. Morton and J. A. Mitchell, "Performance of 931-A Type Multiplier in a Scintillation Counter," RCA Review, Vol. 9, p. 632, December, 1948.

George A. Morton, "Photomultipliers for Scintillation Counting," RCA Review, Vol. 10, p. 531, December, 1949.

J. A. Rajchman and R. L. Snyder, "An Electrostatically Focused Multiplier Phototube," Electronics, Vol. 13, p. 20, December, 1940.

H. Bruining, Physics and Applications of Secondary Electron Emission (McGraw-Hill Book Company, Inc., New York, 1954), pp. 78-81.